INTERNATIONAL JOURNAL OF BUILT ENVIRONMENT AND SUSTAINABILITY
Published by Faculty of Built Environment, Universiti Teknologi Malaysia
Website: http://www.ijbes.utm.my
IJBES 2(1)/2015, 48-61

Impact of Urban Heat Island under the Hanoi Master Plan 2030 on Cooling Loads in Residential Buildings

Tran Hoang Hai Nam[1], Tetsu Kubota[2] and Andhang Rakhmat Trihamdani[1]
[1]Graduate Student, Graduate School for International Development and Cooperation, Hiroshima University
[2]Associate Professor, Graduate School for International Development and Cooperation, Hiroshima University
Email: tranhoanghainam@gmail.com

History:
Received: 24 December 2014
Accepted: 30 December 2014
Available Online: 30 January 2015

Keywords:
Urban heat island; Energy consumption; Air-conditioning; Cooling load; Master Plan

Contact Number:
+ 84-09828 09626 (Nam)

ABSTRACT

This study aims to evaluate the influence of urban heat island (UHI) under the Hanoi Master Plan 2030 on the energy consumption for space cooling in residential buildings. The weather conditions under the current and future status (master plan condition) simulated in the previous study (Trihamdani et al., 2014) were used and cooling loads in all the residential buildings in Hanoi over the hottest month were estimated under the simulated current and future conditions by using the building simulation program, TRNSYS (v17). Three most typical housing types in the city were selected for the simulation. The cooling loads of respective housing types were obtained in each of the districts in Hanoi. The results show that the total cooling loads over June 2010 is approximately 683 Terajoule (TJ) under the current status, but it is predicted to increase to 903 TJ under the master plan condition. The increment is largely due to the increase in number of households (203 TJ or 92%), but partially due to the increase in urban temperature, i.e. UHI effect (17 TJ or 8%). The increments in new built-up areas were found to be larger than those in existing built-up areas. The cooling load in apartment is approximately half of that in detached house, which is approximately half of that in row house. Moreover, it was seen that although sensible cooling loads increased with the increase in outdoor temperature, the latent cooling loads decreased due to the decrease in absolute humidity and the increase in air temperature.

1. Introduction

In the context of rapid population growth and urbanization in recent years, Southeast Asian countries are facing many urban environmental issues. One of them is urban heat island (UHI) phenomenon which alters urban climate compared to the surrounding rural areas. The UHI intensity (UHII) is expected to increase further in the future because most of the countries in this region plan to increase their urban population dramatically in line with their proposed large-scale master plans. Consequently, the increase in urban temperatures due to UHI would lead to increase in energy consumption for space cooling in buildings in particular because of the year-round hot-humid climates. In Vietnam, the Government implemented the Hanoi Master Plan 2030 in June 2011. The master plan aims to develop Hanoi into a civilized and modernized capital city with abundant green spaces. Although the environmental impact assessments in the master plan were conducted for several issues such as soil pollution, air pollution, water quality and eco-systems, it did not take into account the influence of UHI phenomenon.

This study aims to evaluate the influence of UHI under the Hanoi Master Plan 2030 on the energy consumption for space cooling in residential buildings of the city. The weather conditions simulated in the previous study (Trihamdani et al., 2014) are used and cooling loads in all the residential buildings in Hanoi over the hottest month are estimated under the simulated current and future conditions by using the building simulation program, TRNSYS (v17). Three most typical housing types in the city were selected for the energy simulation. The cooling loads of respective housing types were obtained in each of the districts in Hanoi.

During the urbanization period from 1980, Hanoi experienced an upward trend in the annual air temperature. Figure 1 shows the annual average air temperature recorded at the three weather stations in Hanoi from 1980 to 2010. Based on the location of stations, Lang, Hadong, Bavi are considered to be urban, sub-urban and rural area respectively. As shown in Figure 1, the average air temperature in Lang (urban) increased by about 1.5 ℃ while those in rural area (Bavi) rose by only 0.5 ℃. In 2010, the air temperature difference reached 2 ℃, which showed the existence of UHI in Hanoi.

Population of Hanoi was over 6.4 million people in 2009 and the urbanization rate was nearly 40.8%. It was forecasted that the population would increase up to 7.3-7.9 million people by 2020 with the urbanization rate of 58-60%. By 2030, its population would reach 9-9.2 million people with urbanization rate of 65-68%. By 2050, the maximum population is forecasted to be 10.8 million people with urbanization rate of 70-80%. Under rapid urbanization that caused massive pressures on resources and the environment, the Vietnam Government officially implemented the Hanoi Master Plan 2030 Vision 2050 in July 2011 (Figure 2). The main target of the master plan is to develop Hanoi to be a Green-Cultured-Civilized-Modern City. Hanoi Capital is developed based on the comprehensive structural plan comprising several urban bunches including the central urban and satellite urban areas. These urban bunches are connected with each

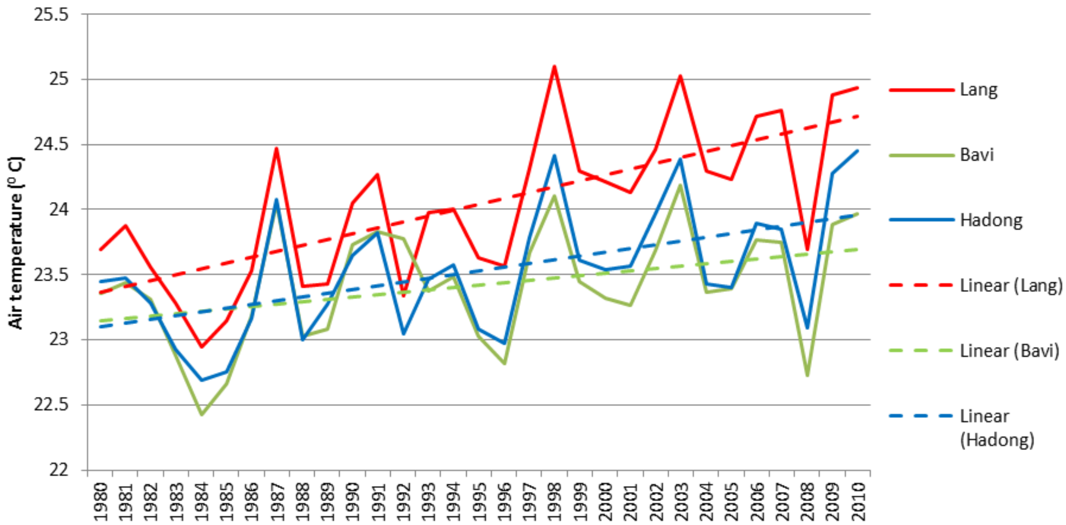

Figure 1: *Annual average air temperature of Hanoi from 1980 to 2010. (Source: Hydro Meteorological Data Center)*

other by a corridor transit system. The master plan also proposed the green space network consisting of the established green corridor, green belt, green buffer and other green spaces. Due to the urban expansion, 28% of the city's natural land will be allocated for the urban construction by 2030. The total build-up areas, therefore, will dramatically increase to almost three times from 46,340 ha (14%) to more than 129,500 ha (39%).

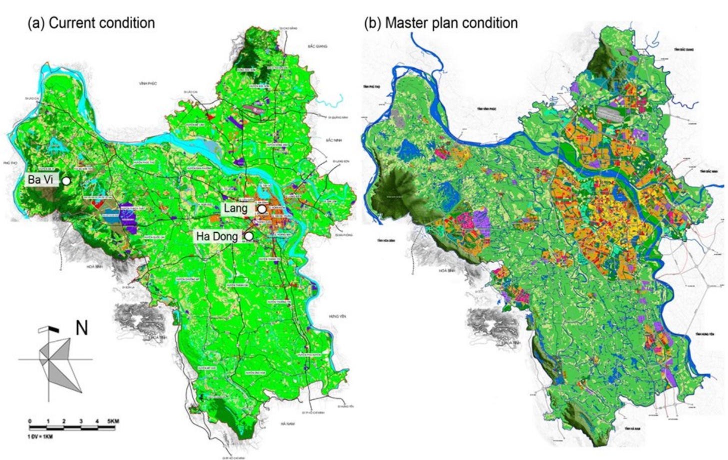

Figure 2: *Land use for current and Master Plan conditions in Hanoi (Source: VIAP)*

Under the rapid economic growth and development, the living standard in Vietnam has been increasing significantly, which results in a large increase in energy consumption. Figure 3 shows the growth of energy consumption in Vietnam, showing the exponential increase. Over the last ten years from 1998 to 2008, the nationwide electricity consumption has increased by 400%. Figure 4 shows the nationwide electricity consumption breakdown by sectors in the three major cities of Vietnam. The electricity consumption for administration and household accounts for the largest proportion in the three cities, which is 54%, 37%, 39%, respectively.

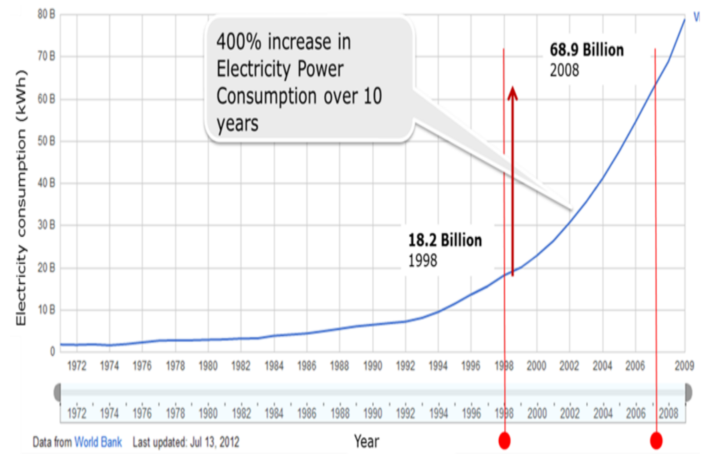

Figure 3: *Growth of energy consumption in Vietnam (Source: World Bank)*

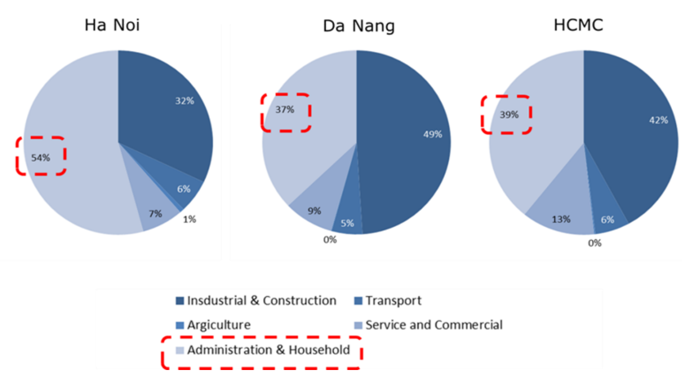

Figure 4: *Electricity consumption in major cities in 2011 (Source: IFC)*

2. Literature Review

The urban geometry and the anthropogenic heat sources are some of the main causes of UHI that increases air temperature in urban areas compared with surrounding rural areas. UHI was first identified by Luke

Howard in 1820 when he found that the air temperature in London city was 3.7°F warmer at night and 0.34°F cooler at day as compared to the country's average temperature. The intensity of UHI differs among cities, of which the greatest intensities are normally observed in densely built-up areas.

The generation of UHI is the mutual response of many factors, both controllable and uncontrollable. These factors are categorized as the temporary effect variables such as wind speed, cloud cover and the permanent effect variables such as green areas, building material, sky view, among others. The anthropogenic heat is generated from human activities such as power plants, automobiles, air conditioners and other sources. Only part of anthropogenic heat directly increase ambient temperature during the daytime, and the rest of heat is absorbed by the complicated structure of urban area including ground surface, walls and roof facets, irrigated and non-irrigated green spaces, pavements, which indirectly heat up the air temperature by releasing the heat during the night-time. The heat released by urban structure depends on the controllable factors such as the sky view factor and, building materials (Memon et al., 2008). The decrease in sky view factor and albedo (i.e. the ratio of reflected radiation and incident radiation), are the two important factors increasing UHI (Giridharan et al., 2004). Little latent heat by evaporation also affects the increase in air temperature especially when urban lacks of vegetation. For example, the evapotranspiration in Tokyo has been decreased by 38% from 1972 to 1995 (Kondoh & Nishiyama, 1999). There are also some other temporary effect variables increasing UHI. For instance, the anticyclone conditions increase UHII (Pongracz et al., 2006). It was reported that wind speed and cloud cover negatively influence UHI (Kim & Baik, 2005; Oke, 1982).

UHI has a long history of study mainly focusing on cities in temperate regions. However, UHI studies in tropical and sub-tropical regions such as Southeast Asia are still limited. Singapore was the first city in which UHI research was conducted in 1964 by Nieuwolt. The measurements taken in the south of Singapore revealed that the city was significantly warmer and drier than rural areas with the maximum UHII of up to 3.5℃ (Nieuwolt, 1966). The distribution of UHI of the entire island was then mapped out by Singapore Meteorological Service (SMS, 1985). Another study conducted in the same city for one year (Chow & Roth, 2006) showed seasonal change of UHII due to the variability of moisture content of rural reference site which is influenced by the precipitation. In Malaysia, the study of UHI in Kuala Lumpur focused on air temperature distributions and analyzed the variability of UHI, which was conducted by Sham in 1972. The study revealed that the UHIs were seen in the built-up areas and mean annual air temperature difference between the urban central and surrounding areas was 1-2 ℃ (Sham, 1986, 1987, 1990). A study in Johor Bahru, the second largest city in Malaysia, also showed that the difference in nocturnal air temperature between city and surrounding areas was 2℃ on rainy days and up to 4℃ on sunny days (Kubota & Ossen, 2009). Although there were very few studies on urban climate conducted in the Philippines (Pereira & Lopez, 2005), the surface temperature in Metro Manila was also derived using remote sensing from 1989 to 2002.

In Vietnam, the research on urban climate has started recently in Ho Chi Minh City. By using thermal remote sensing and processing the Landsat 7 ETM image, the study showed the correlation between various land covers and urban surface temperature. Industrial areas were found to have highest surface temperature (35 ℃ - 39 ℃) followed by built-up areas. Areas covered with vegetation were found to have lower surface temperature of about 24 ℃ - 28 ℃ (Van & Bao, 2006). The UHI in Ho Chi Minh City was confirmed again in another study using data derived from satellite images obtained from 1989 to 2006. The impervious surface and radiant surface temperature were mapped out showing the expansion of built-up area by 6.5 times from 1989 to 2006, and the air temperature of urban areas ranged from 36 ℃ to 40 ℃ with the maximum air temperature of 45 ℃ in industrial areas (Van & Bao, 2010).

A preliminary UHI study in Hanoi was conducted in 2012 to estimate the UHI effect due to land use change proposed by the Hanoi Master Plan (Phuong, 2012). The above study was followed by Trihamdani (2014), which focused especially on the cooling effects of the green space network proposed in the Hanoi Master Plan, by conducting numerical experiments using meteorological model (WRF). Based on the results, the peak air temperature in the daytime in the master plan condition was predicted to maintain almost the same level as the current condition (up to 1℃ higher). However, high air temperature areas, with temperature of 40-41℃, would expand widely in the planned built-up areas. Simulated nocturnal air temperature increased by up to 3-4℃ over the expanded built-up areas. The wind speed in expanded built-up areas was also weaker than those over green spaces. The region where the southerly wind comes during night-time was cooler compare to other regions. The results also showed that the green strategies proposed in the master plan largely reduced the air temperature within the green areas during night-time but not an assurance for cooling all of the built-up areas. Figures 5 and 6 show the air temperature distribution in current condition and master plan condition at 1 am and 4 pm, respectively.

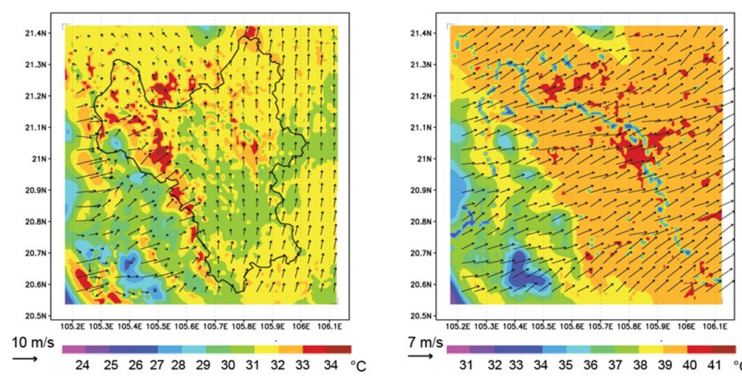

Figure 5: *The temperature distribution in current condition at 1AM and 4PM*

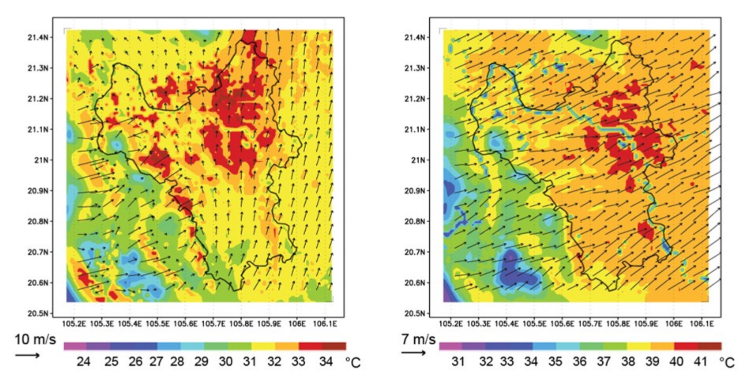

Figure 6: *The temperature distribution in master plan condition at 1AM and 4PM*

Generally, in the high latitude cities where the temperature is cooler, the UHI could positively impact the energy consumption because it can reduce the heat loads. However, in the mid and low latitude cities, the UHI only brings negative impacts. The negative impacts of UHI include the deterioration of living environment and increase in energy consumption (Konopacki et al., 2002), elevation of ground level ozone (Rosenfeld et al., 1998) and to a certain extent, an increase in mortality rates.

To evaluate the impacts of UHI on energy consumption, many studies have been conducted in different cities such as Athens (Assimakopoulos et al., 2007; Hassid et al., 2000; Santamouris et al., 2001), Taipei (Hsieh et al., 2007) and London (M. Kolokotroni et al., 2006; Maria Kolokotroni et al., 2007). However, the number of studies is still insufficient because different cities have different climate condition, building style and so on. Therefore, it is necessary to conduct the UHI evaluation for many cities worldwide. The methodologies to evaluate the impact of UHI on energy consumption also vary among studies. In Osaka City, a study simulated residential energy consumption under various behaviors of inhabitants and estimated residential energy consumption of the entire city. However, they did not show the actual temperature increase by UHI (Shimoda et al., 2007). Moreover, most of the studies were based on air-conditioning load that depends on many input parameters (e.g., wall insulation, type of air conditioner, ratio of windows on walls, etc.) while building types differ from each other among cities. Some studies have investigated the temperature sensitivity for energy consumption to evaluate climate condition as well as to predict the energy demand (Fung et al., 2006; Mirasgedis et al., 2006; Psiloglou et al., 2009; Sailor, 1997). These studies used data from supply-side so that the temperature distribution was not considered. Hence, it is necessary to take into consideration the spatial and temporal distribution of both energy consumption and indoor air temperature (Hirano & Fujita, 2012).

3. Methods

3.1. *Classification of residential buildings in Hanoi*

In order to determine the typical houses that will be used for the energy simulations, we collected 400 drawings of residential buildings in Hanoi from various sources such as architectural consultant studios, construction companies and real estate companies. In Hanoi, row house, detached house and apartment are the most typical housing types. The drawings collected include floor plans, perspective view, and basic information such as year of construction, and site location, etc.

Figure 7(a) shows a sample of floor plan of row house. All drawings of row house were further classified into several groups by considering the design elements that may influence their indoor thermal environments, such as existence of balcony and courtyard or light well, etc. The room arrangement was also taken into account in the classification. In Hanoi, most of the houses tend to install air-conditioners in their master bedrooms. Therefore, it is important to classify the row houses according to the arrangement of master bedroom. We found that, in general, the row houses have the master bedroom on the second floor, facing the main street, whereas living room, kitchen and dining room are located on the ground floor.

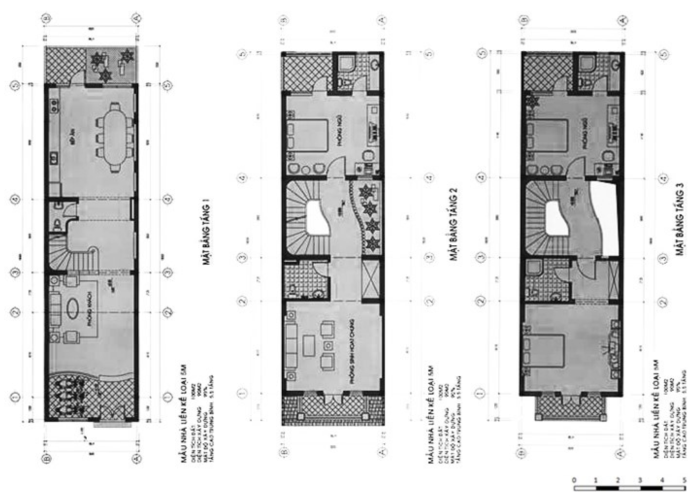

Figure 7(a): *Sample of row house floor plan*

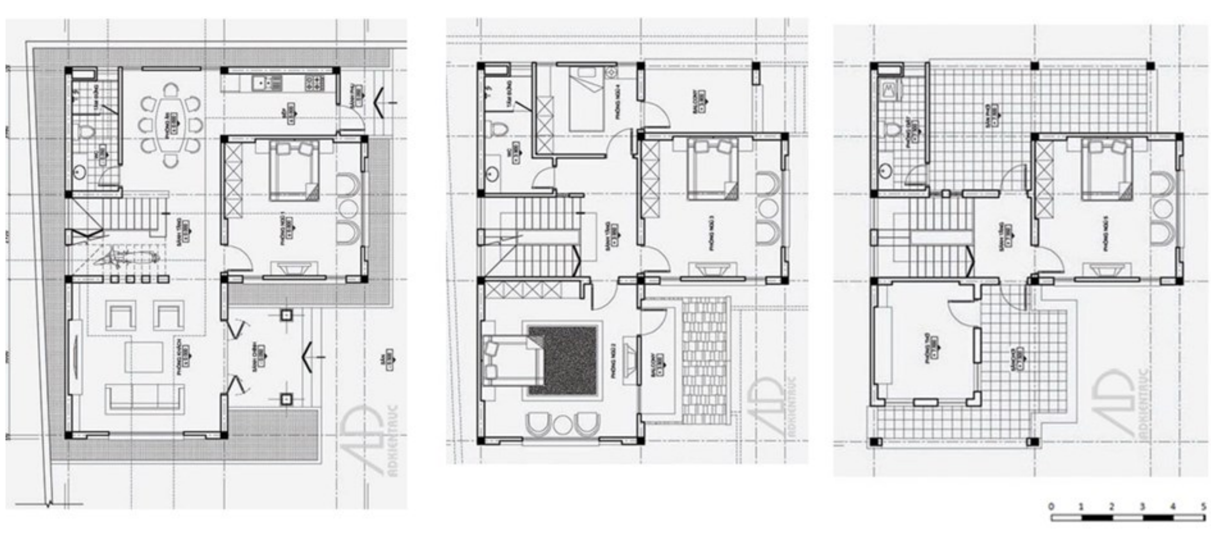

Figure 7(b): *Sample of detached house floor plan*

The drawings of detached house are more diversified compared with row houses. This is mainly because detached houses normally have larger site areas and there are more open spaces around the houses, and therefore they have more variations of house designs. However, the air-conditioners are still typically installed in the master bedroom. Most of the master bedrooms were found to be located on the second floor, while the first floor is used for living room, kitchen and dining room. It is predicted that the envelopes of master bedroom and existence of balcony would particularly influence its indoor thermal conditions. Generally, each of the master bedrooms has one to three outer walls facing the external environments. The more outer walls it has, the more the room is influenced by the outdoor conditions. Figure 7(b) shows a sample of detached houses in which the master bedroom with a balcony is located on the second floor. For apartments, the classification was made also based on the arrangement of master bedroom. Figure 7(c) shows a sample of apartments and its location in the apartment block. Most of the apartment units have only one outer wall that is exposed to the outdoors.

Figure 7(c): Sample of apartment floor plan

Table 1: *Classification of residential buildings in terms of floor area and room arrangement*

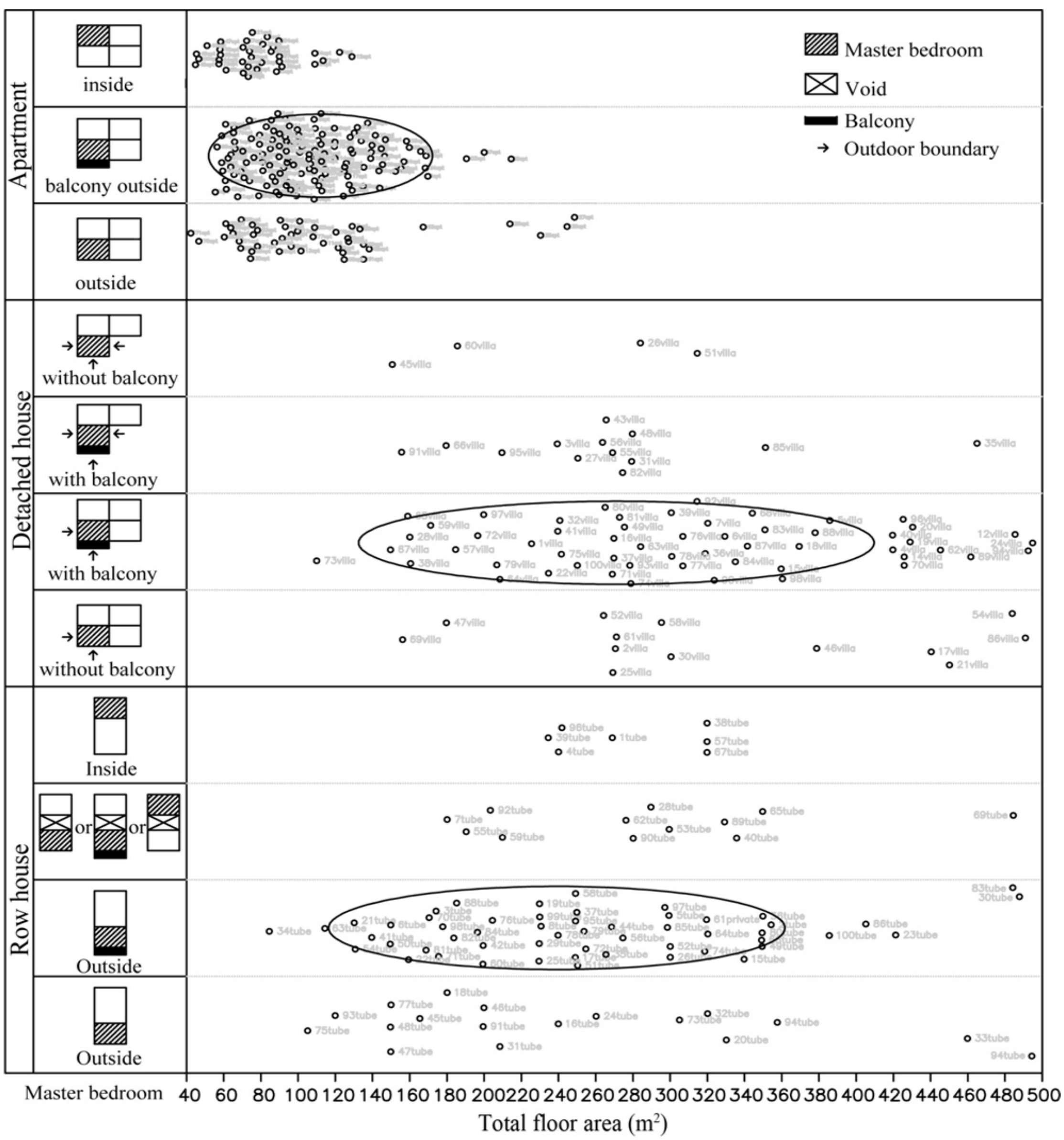

Table 1 shows the classification of the above three types of houses (i.e. row house, detached house and apartment) in terms of total floor area, room arrangement and the existence of balcony and void space. As shown, the total floor area of row houses ranges from 120-360m^2, whereas that for detached house is from 140-400m^2 and that for apartment is from 60 to 60m^2 respectively. As a result, the most typical row house was determined as the one that has a balcony but no void space. The average total floor area of the typical row houses is 240m^2. Meanwhile, the most typical detached house was determined to be the one that has the master bedroom on the second floor, facing the main street outside. The master bedroom has two outer walls with a balcony with the average total floor area of 280m^2. The average total floor of the most typical apartment is smaller than other housing types, which is around 100m^2, and it has the master bedroom with two outer walls with a balcony.

After determining the most typical houses for respective housing types, their three dimensional (3D) models were formed for the following simulations. These 3D models were drawn by using the Google Sketchup program and the Trnsys3d plugin.

3.2. Input weather conditions used for simulations

The weather data that will be used for the following building simulations were obtained from the previous study (Trihamdani et al., 2014). As explained before, the above study investigated the UHI effect in Hanoi under present land use condition as well as under those conditions proposed by the Hanoi Master Plan 2030 through numerical simulations. The simulated weather data include air temperature, relative humidity, wind speed, wind direction, solar radiation and air pressure. Each data file represents the weather data for 1 x 1 km2. Both current and master plan conditions have equal number of 9801 files in the entire Hanoi city.

Basically, the total cooling load of the whole Hanoi city was estimated through multiplying the cooling load of respective housing types by the number of households. Since the number of households is given by respective administrative districts (29 districts) in Hanoi, the simulation of energy consumption needs to be conducted separately for each district (Figure 8). For the above reason, we averaged the weather data

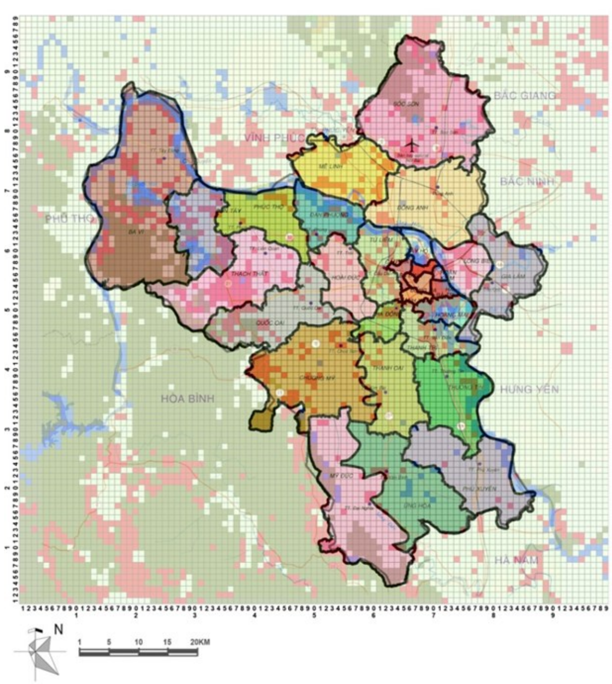

Figure 8: *Overlay of built-up map and district map*

obtained from Trihamdani et al. (2014) for each of the districts in current condition and master plan condition, respectively. Thus, a total of 29 weather files were generated through this process.

3.3. Simulation conditions

Time period of simulation is 1 month starting from 1 June 2010 with the simulation interval time of one hour. The latitude of the buildings is set to be 21'03N. Figure 9 shows the results of tentative simulation of a sample building (row house) in 8 different orientations. As expected, the building facing to the West and North-West recorded higher average indoor air temperatures for one month, while those facing to the East, South-East and South obtained the lower average air temperatures. Based on the above result, the orientation of all buildings in the following simulations was set to be the one that represents the mean indoor air temperature among 8 orientations, which is the North orientation. It was assumed in the simulations that the air-conditioners are used only in the master bedroom during night-time from 10 pm to 3 am (5 hours/day) with the set-point temperature of 26 °C. These conditions were determined based on the survey results conducted by Phan & Yoshino (2010). Moreover, to estimate latent cooling load, the dehumidification function was assumed with the set-point relative humidity of 60%. The internal heat gains were taken into account based on the assumption that there are two occupants (sedentary conditions) with light work and one television in the master bedroom. Furthermore, the future number of households and percentage of the three housing types projected in the master plan shown in table 2 were used for the cooling load estimations.

3.4. Validation

The validation of simulation results was made by using the results of field measurements that were carried out in Da Nang city by Nguyen (2013). The measurements were conducted in a row house, a detached house, and an apartment for one month, respectively, in May 2012 (Figure 10). Although these houses are not located in Hanoi city, their architectural styles and construction materials are similar with those in Hanoi.

The row house was built in 2003. During the field measurement in 2012, the house was unoccupied from 1st to 20th May, but was occupied by 3 family members from 20th to 31st May. The detached house was occupied by a family of 4 during the whole measurement period. The air conditioner was in free running mode during the period of measurement. The apartment is located on the 4th floor of 7-storey apartment block constructed in 2010. During the measurement period, it was occupied by 2 persons. The openings of row house were controlled by the author differently in 3 sub-periods. From 1st to 9th May, all openings and door were closed. They were all opened from 10th to 19th (except entrance doors). From 20th to 31st, under the occupancy, they were manually controlled corresponding with outdoor conditions. In both detached house and apartment, the information of occupancy was gathered by questionnaires. Their openings were freely controlled by the occupants and were almost opened throughout the day.

The measured three houses were modeled by using the Google Sketchup and Trnsys3d plugin (Figure 11). The wall thickness in the row house is 110 mm, whereas those in detached house and apartment are 220 mm. In the row house, the material for foundation, structure and floor is reinforced concrete, while those for roof are metal color sheet and PVC ceiling panel. The single glazing-steel frame is applied for openings. The surrounding conditions including two other adjacent buildings and a tree

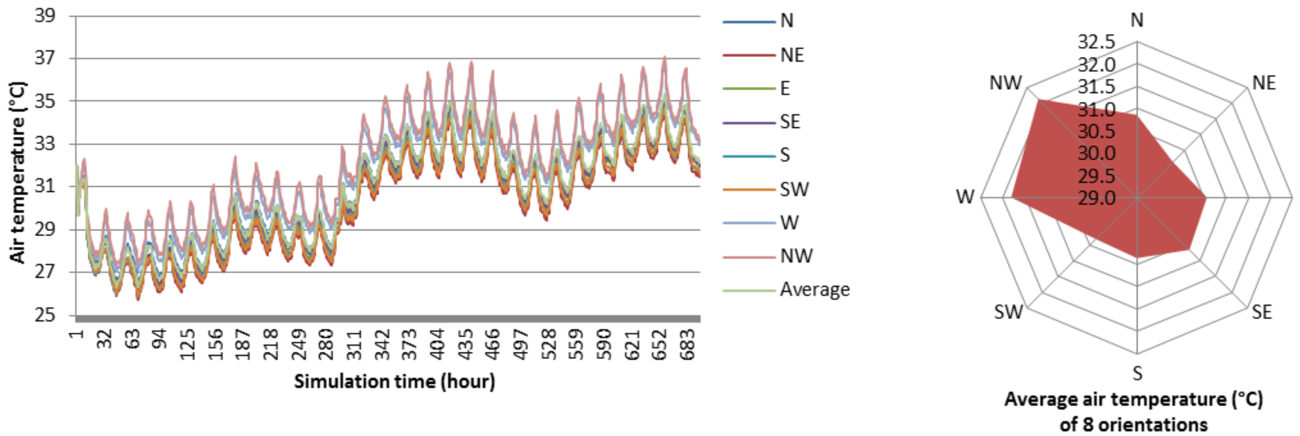

N	NE	E	SE	S	SW	W	NW	Mean
30.85	30.13	30.57	30.66	30.36	30.32	31.82	32.12	30.85

Figure 9: *Tentative simulation results in 8 orientations*

Table 2: *Number of household in respective district (Source: VIAP)*

		Current			Master Plan		
	District	**Row house**	**Detached house**	**Apartment**	**Row house**	**Detached house**	**Apartment**
Hanoi 1	Quận Đống Đa	61149	3007	21977	87600	4308	20423
	Quận Ba Đình	46215	2273	3390	60740	2987	3279
	Quận Hoàn Kiếm	31336	1541	1009	40504	1992	847
	Quận Hai Bà Trưng	58222	2863	8275	75309	3704	10573
	Quận Long Biên	47902	2356	3462	60986	2999	7084
	Quận Tây Hồ	28598	1406	1548	37862	1862	2018
	Quận Hoàng Mai	59159	2909	16563	72770	3579	27676
	Quận Cầu Giấy	36208	1781	16116	46202	2272	23105
	Quận Thanh Xuân	34736	1708	17004	46175	2271	22263
Hanoi 2	Quận Hà Đông	51151	2516	1164	54930	2701	14907
	Thị xã Sơn Tây	14383	707	206	17065	839	2332
	Huyện Thạch Thất	1119	55	0	1469	72	13
	Huyện Sóc Sơn	664	33	7	871	43	19
	Huyện Quốc Oai	2675	132	0	3546	174	0
	Huyện Ba Vì	2655	131	0	3519	173	0
	Huyện Từ Liêm	6369	313	22	8212	404	262
	Huyện Đan Phượng	1818	89	0	2410	119	0
	Huyện Thanh Trì	3100	152	29	4036	198	112
	Huyện Đông Anh	4997	246	22	6583	324	64
	Huyện Gia Lâm	7364	362	87	9621	473	252
	Huyện Chương Mỹ	8265	406	0	10857	534	103
	Huyện Hoài Đức	1128	55	0	1483	73	11
	Huyện Mê Linh	5375	264	0	7066	347	55
	Huyện Mỹ Đức	1339	66	0	1775	87	0
	Huyện Phú Xuyên	3077	151	0	4078	201	0
	Huyện Phúc Thọ	1549	76	0	2045	101	8
	Huyện Thanh Oai	1289	63	0	1709	84	0
	Huyện Thường Tín	1513	74	0	1998	98	8
	Huyện Ứng Hoà	2797	138	0	3708	182	0

in front of master bedroom were considered in the model. In the detached house, the material for foundation and structure is reinforced concrete, whereas those for roof are metal color sheet and reinforced concrete ceiling. The single glazing-wooden frame is adopted for openings. Except for a tree behind the house, all other surrounding elements were not taken into account. As shown in Figure 11(c), the 3D model of apartment represents the whole apartment block. Almost all the construction elements of apartment, such as foundation, structure, roof, and floor, are reinforced concrete. All external and internal walls are made up of solid brick and the single glazing-aluminum frames are used for openings. The outdoor condition surrounding the apartment block was not modeled.

Where Lis is the ith simulated value, Lim is the ith measured value and N is the total number of data pairs. Generally, the better prediction means smaller error.

In this study, two statistical error tests were used to check the deviations of simulation results: they are the Normalized Mean Bias Error (NMBE) and Coefficient of Variation of Root Square Mean Error CV(RMSE). These statistical error tests have been applied in some validation guidelines such as ASHRAE guideline 14 (ASHRAE, 2002), ASHRAE

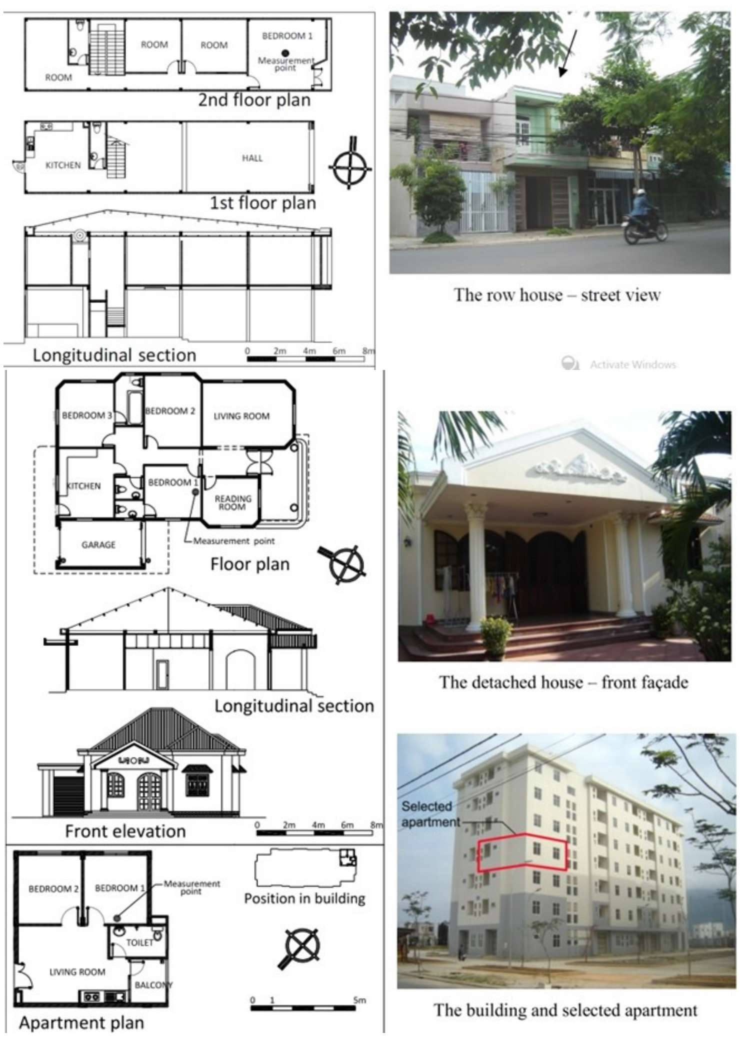

Figure 10: *Residential buildings used in field measurement (Source: Nguyen 2013)*

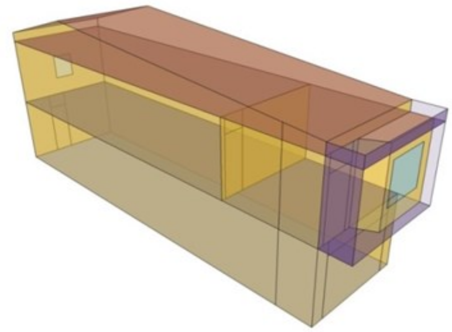

Figure 11(a): *3D model of row house for validation*

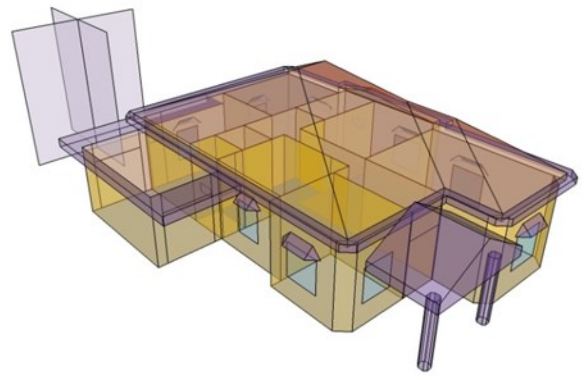

Figure 11(b): *3D model of detached house for validation*

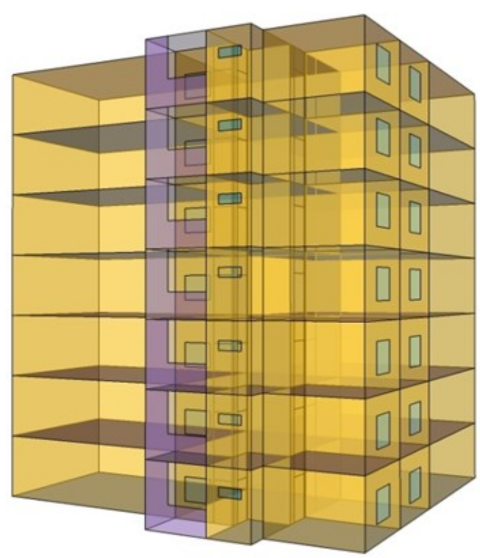

Figure 11(c): *3D model of apartment for validation*

Handbook of Fundamentals (ASHRAE, 2009) and other existing literature (Jiang, 2009). The said statistics were calculated as follows:

$$MBE = \sum_{i=1}^{N} (L_{is} - L_{im})/N \qquad (1)$$

$$RMSE = \sqrt{\sum_{i=1}^{N} \frac{(L_{is} - L_{im})^2}{N}} \qquad (2)$$

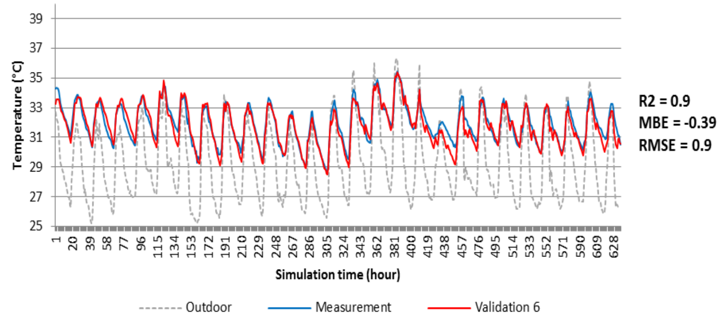

Figure 12: Comparison between observed and simulated air temperature in row house

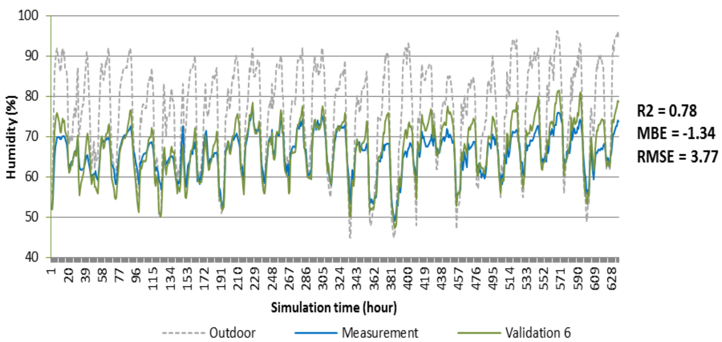

Figure 13: Comparison between observed and simulated relative humidity in row house

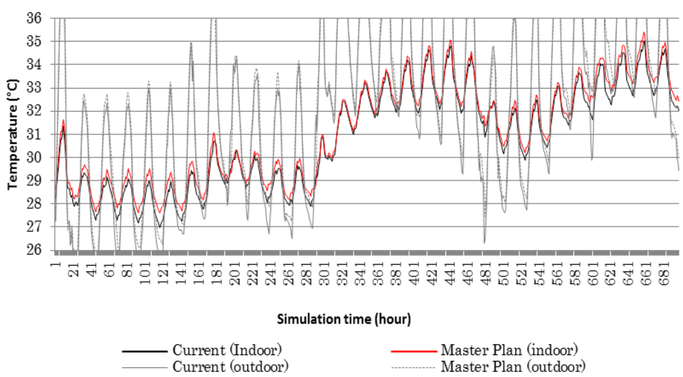

Figure 14: Simulation results of before and after implementation of the Hanoi Master Plan (Simulation of Row-house in Hoai Duc district)

Due to the space constraint, we only show the validation result of row house (Figures 12 and 13). The validation was conducted in the master bedroom on the second floor. There are more than 30 validation runs during the progress, and the results obtained good agreements in terms of both air temperature and relative humidity. As shown, R2-value was 0.90 with MBE of -0.39 and RMSE of 0.90 for air temperature, whereas those for relative humidity are 0.78, -1.34 and 3.77, respectively. These statistical figures are satisfactory according to the guidelines of (ASHRAE, 2009). The validation results were also satisfactory for both the detached house and apartment.

4. Results and discussion

4.1. Sensible cooling load per household

The monthly sensible cooling loads in June 2010, which was the hottest month over the period of 2000-2012, under the current conditions and master plan conditions are estimated. The total monthly cooling loads in all the residential buildings for the two conditions are calculated through multiplying the simulated cooling loads of respective building types by the number of households. Figure 14 illustrates one of the examples of simulation results for a row house located in Hoai Duc district of Hanoi. As described in the previous study (Trihamdani et al., 2014), nocturnal outdoor air temperatures are predicted to increase in particular after the implementation of the master plan. Accordingly, indoor temperature is increased by approximately 1 °C at night. The increase in the nocturnal temperature results in the increase in the cooling loads because air-conditioners are used during the night-time as described before. As such, the simulations of three base models were run in 29 districts respectively (A total of 174 simulations were run for current and master plan conditions).

Table 3 summarizes the calculation results of monthly sensible cooling loads per household by the three housing types and the two different districts (i.e. existing built-up districts and new built-up districts). The new built-up districts are the areas in which built-up areas are largely expanded due to the master plan. In general, the sensible cooling loads in row house and detached house are approximately 1.5 times larger than those in apartment. As shown, the monthly sensible cooling load per household are predicted to increase by 33-34 MJ in the case of row house and detached house for existing districts, while those for apartment are 25 MJ on the average. In contrast, for the case of new built-up area, the corresponding increments for row house and detached house are 53-54 MJ and those for apartment are 39 MJ. As expected, the increments in the new built-up districts are slightly large because of the larger increase in the outdoor air temperature.

4.2. Latent cooling load per household

Table 4 summarizes the calculation results of monthly latent cooling loads per household under the current condition and master plan conditions. As shown, although outdoor air temperatures were increased after the implementation of the master plan, the absolute humidity is declined due to the effects of UHI. Thus, the outdoor relative humidity generally drops relatively largely in both existing built-up areas and new built-up areas. For these reasons, the latent cooling loads are reduced in all the cases as shown in Table 4. In contrast with the sensible cooling load, the latent cooling loads in row house are approximately 2 times larger than those in detached house, while those in detached house are approximately 2 times larger than those in apartment. As shown, the monthly latent cooling loads per household are predicted to decrease by 22-32 MJ in the case of row house, by 10-15 MJ in detached house, and by 5-7 MJ in apartment, respectively.

4.3. Total cooling load per household

The total monthly cooling loads (sensible + latent) per household under current condition and master plan condition are summarized in Table 5. The increase in cooling load under master plan condition still can be seen but it is not large because of the reduction in latent cooling loads. In the existing built-up areas, the monthly cooling loads per household

Table 3: Sensible cooling load in one household

	Outdoor temperature	Row house	Detached house	Apartment
Existing built-up area	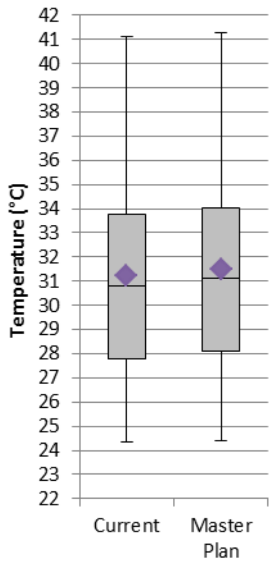	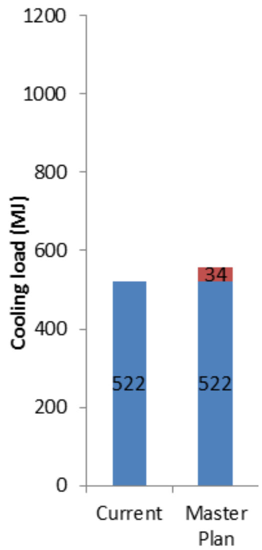	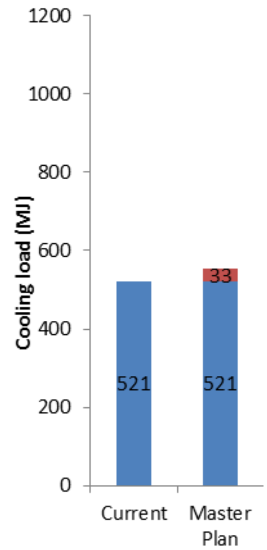	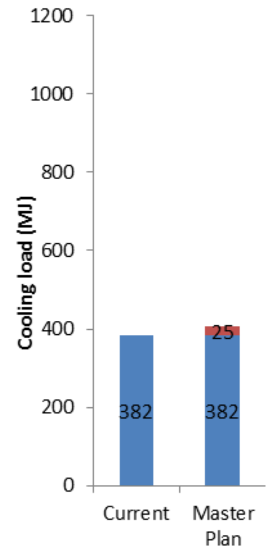
New built-up area	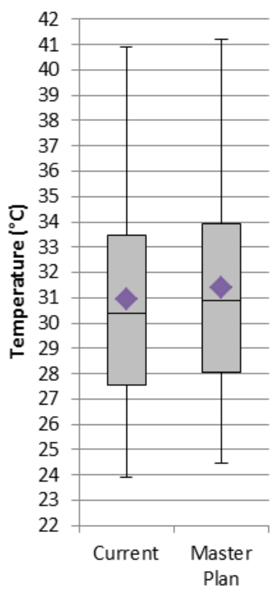	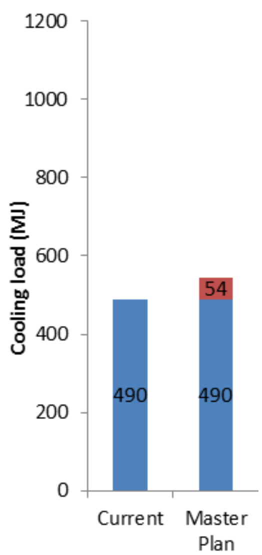	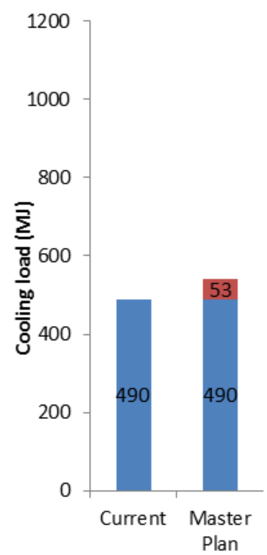	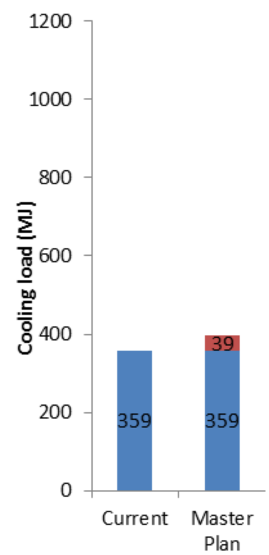

are predicted to increase by 13 MJ in the case of row house, by 23 MJ in detached house, and by 20 MJ in apartment on average, respectively. In contrast, in the case of new built-up areas, the corresponding increase for row house, detached house and apartment are 22 MJ, 37 MJ and 32 MJ, respectively.

4.4. Total cooling load of residential buildings in Hanoi

The total accumulated cooling loads in each district were calculated by multiplying the per-household cooling load by the number of households (row house, detached house and apartment). Then, the total accumulated cooling loads in all the residential buildings in Hanoi under the two conditions were estimated by summing cooling loads of all districts (29 districts) (Figure 15). As shown, the increments can be divided into two proportions (i.e. the increment due to the increase in number of households, and that caused by the increase in outdoor air temperature (UHI)).

Under the current condition, the total monthly cooling load was calculated as about 683 TJ. This amount is predicted to increase to 903 TJ under the master plan condition. It can be seen that the increase in the number of households would increase the total cooling loads largely (203 TJ/month), but the UHI effects would also indirectly increase the cooling loads in residential buildings by 17 TJ/month.

Table 4: Latent cooling load in one household

	Absolute humidity	Row house	Detached house	Apartment
Existing built-up area	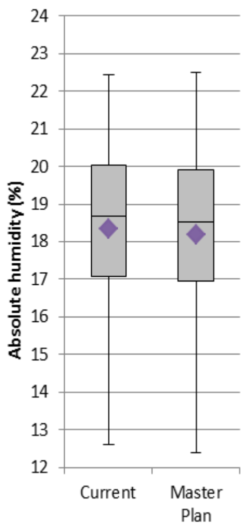	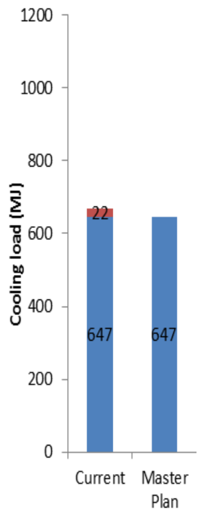	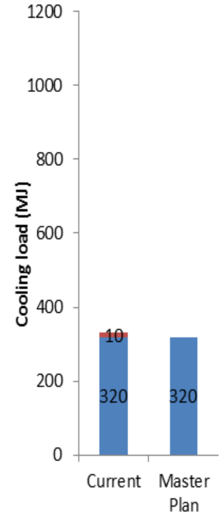	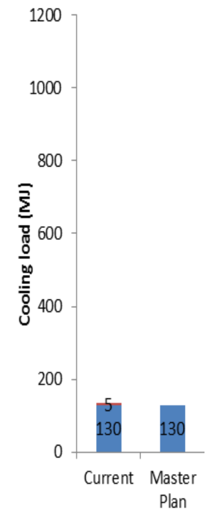
New built-up area	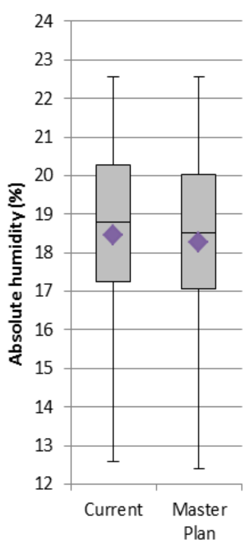	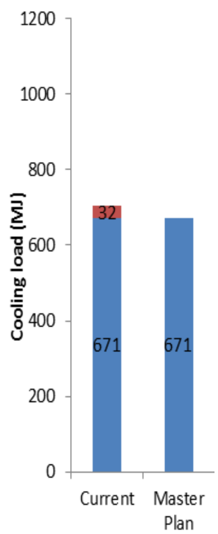	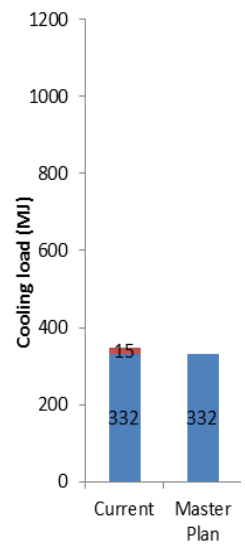	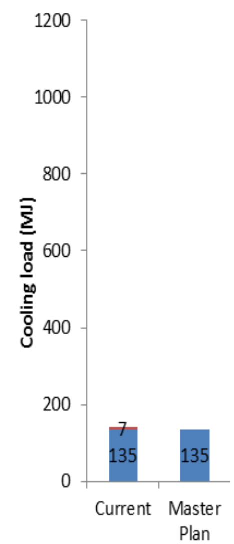

5. Conclusions

This study estimated the total cooling loads in all the residential buildings in Hanoi under the current condition and the future master plan condition, based on the numerical simulations. The simulations were run separately for different housing types (row house, detached house, and apartment) in respective districts in Hanoi. The results in existing built-up areas and new built-up areas were also compared to figure out the difference of UHI effects. The main findings are as follows:

The total cooling loads, including sensible and latent loads, of all the residential buildings in Hanoi over June 2010 is approximately 683 TJ under the current condition, but it is predicted to increase to 903 TJ after the implementation of the Hanoi Master Plan 2030.

The increment is largely due to the increase in number of households in the future (203 TJ or 92%), but partially due to the increase in urban temperature, i.e. UHI effect (17 TJ or 8%).

The increments in new built-up areas were found to be larger than those in existing built-up areas. Generally, the monthly average cooling load in row house was approximately 50% larger than that in detached house, which was also about 50% larger than that in apartment. This can be explained by the relatively high latent cooling loads observed in the row houses.

Table 5: *Total cooling load in one household*

	Row house	Detached house	Apartment
Existing built-up area	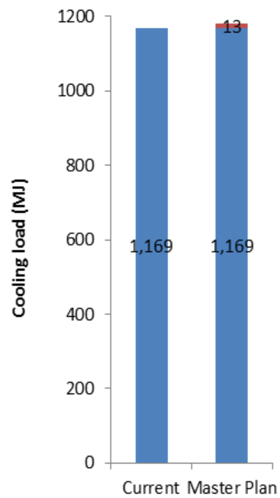	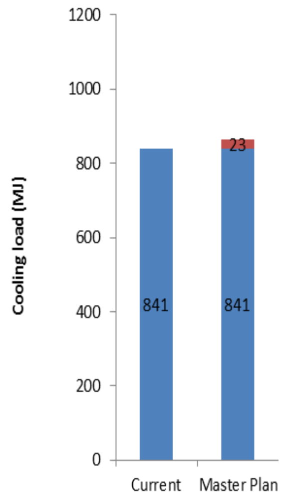	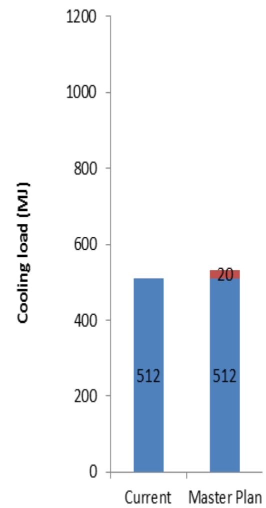
New built-up area	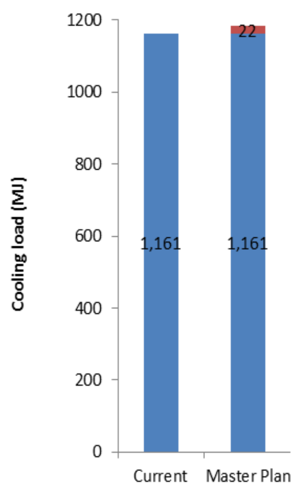	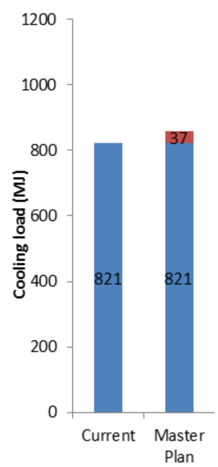	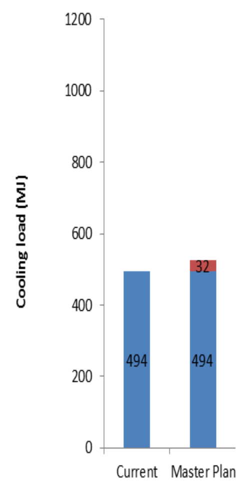

The sensible cooling loads were increased in all the housing types after the implementation of master plan due to the increase in outdoor air temperature. However, the absolute humidity was declined due to the UHI effect together with the increase in air temperature. This resulted in the decrease in latent cooling loads in all the housing types. As a consequence, the decrease in latent cooling loads offset the increase in total cooling loads.

UHI would become a crucial problem in the rapid growing cities particularly in hot-humid climate regions. In Vietnam, the implementation of Master Plan 2030 would accelerate UHI effects and increase energy demand significantly. This study deals with only residential buildings, and therefore it is important to cover the other building types such as commercial buildings in the future study. Moreover, this study estimates the cooling loads in the master bedrooms under the assumption that air-conditioning is used during night-time with closed windows. The increase in outdoor air temperature increases the cooling loads as the present paper showed, but on the other hand, it significantly affects the potential of night ventilation (Santamouris, 2001). Further study is required to analyze the effects of UHI on the night ventilation potentials in Hanoi.

Acknowledgements

The kind support from Vietnam Institute of Architecture, Urban and Rural Planning is highly acknowledged. We also deeply thank Dr. Anh Tuan Nguyen, Ms. Pham Thi Nham and those who were involved in this research. This research was supported by a grant from Mitsui Co., Ltd. Environment Fund.

References

ASHRAE. (2002). ASHRAE Guideline 14-2002: Measurement of energy and demand savings. Atlanta GA: ASHRAE, Inc.

ASHRAE. (2009). ASHRAE handbook of Fundamentals. Atlanta GA: ASHRAE, Inc.

Assimakopoulos, M. N., Mihalakakou, G., & Flocas, H. A. (2007). Simulating the thermal behavior of a building during summer period in the urban environment. Renewable Energy, 32(11), 1805–1816. doi:10.1016/j.renene.2006.08.003

Chow, W. T. L., & Roth, M. (2006). Temporal dynamics of the urban heat island of Singapore, 2260(July), 2243–2260. doi:10.1002/joc

Fung, W., Lam, K., Hung, W., Pang, S., & Lee, Y. (2006). Impact of urban temperature on energy consumption of Hong Kong. Energy, 31 (14), 2623–2637. doi:10.1016/j.energy.2005.12.009

Giridharan, R., Ganesan, S., & Lau, S. S. . (2004). Daytime urban heat island effect in high-rise and high-density residential developments in Hong Kong. Energy and Buildings, 36(6), 525–534. doi:10.1016/ j.enbuild.2003.12.016

Hassid, S., Santamouris, M., Papanikolaou, N., Linardi, A., & Klitsikas, N. (2000). The effect of the Athens heat island on air conditioning load, (June 1997).

Hirano, Y., & Fujita, T. (2012). Evaluation of the impact of the urban heat island on residential and commercial energy consumption in Tokyo. Energy, 37(1), 371–383. doi:10.1016/j.energy.2011.11.018

Hsieh, C.-M., Aramaki, T., & Hanaki, K. (2007). The feedback of heat rejection to air conditioning load during the nighttime in subtropical climate. Energy and Buildings, 39(11), 1175–1182. doi:10.1016/ j.enbuild.2006.06.016

Jiang, Y. (2009). Estimation of monthly mean daily diffuse radiation in China. Applied Energy, 86(9), 1458–1464. doi:10.1016/ j.apenergy.2009.01.002

Kim, Y., & Baik, J. (2005). Spatial and Temporal Structure of the Urban Heat Island in Seoul, (1973), 591–606.

Kolokotroni, M., Giannitsaris, I., & Watkins, R. (2006). The effect of the London urban heat island on building summer cooling demand and night ventilation strategies. Solar Energy, 80(4), 383–392. doi:10.1016/j.solener.2005.03.010

Kolokotroni, M., Zhang, Y., & Watkins, R. (2007). The London Heat Island and building cooling design. Solar Energy, 81(1), 102–110. doi:10.1016/j.solener.2006.06.005

Kondoh, A., & Nishiyama, J. (1999). Changes in hydrological cycle due to urbanization in the suburb of Tokyo Metropolitan area, Japan. Advances in Space Research, 26(7), 1173–1176. doi:10.1016/S0273-1177(99)01143-6

Konopacki, S., Akbari, H., Group, H. I., Energy, E., Division, T., & Berkeley, L. (2002). Energy Savings of Heat-Island Reduction Strategies in Chicago and Houston (Including Updates for Baton Rouge , Sacramento , and Salt Lake City), (February).

Kubota, T., & Ossen, D. R. (2009). Spatial characteristics of Urban Heat Island. In The 3rd Symposium of South East Aisan Technical University Consortium (SEATUC).

Memon, R. A., Leung, D. Y. C., & Chunho, L. (2008). A review on the generation, determination and mitigation of urban heat island. Journal of Environmental Sciences (China), 20(1), 120–8. Retrieved from http://www.ncbi.nlm.nih.gov/pubmed/18572534

Mirasgedis, S., Sarafidis, Y., Georgopoulou, E., Lalas, D., Moschovits, M., Karagiannis, F., & Pakakonstantinou, D. (2006). Models for mid-term electricity demand forecasting incorporating weather influences. Energy, 31(2-3), 208–227. doi:10.1016/j.energy.2005.02.016

Nguyen, A.-T. (2013). Sustainable housing in Vietnam: Climate responsive design strategies.

Nieuwolt, S. (1966). The urban microclimate of Singapore. J. Trop. Geog, 22, 30–37.

Oke, T. (1982). The energetic basis of the urban heat island. Quarterly Journal of the Royal Meteorological Society, 108, 1–24.

Pereira, R. A., & Lopez, E. D. (2005). Characterizing the Spatial Pattern Changes of Urban Heat Islands in Metro Manila Using Remote Sensing Techniques, 25(1), 15–34.

Phan, T. V. Le, & Yoshino, H. (2010). Survey on Energy Consumption and Environment of Urban Residential Buildings in Vietnam, 1–12.

Phuong, T. (2012). Urban Heat Island effects due to land use change proposed by The Hanoi Master Plan.

Pongracz, R., Bartholy, J., & Dezso, Z. (2006). Remotely sensed thermal information applied to urban climate analysis. Advances in Space Research, 37(12), 2191–2196. doi:10.1016/j.asr.2005.06.069

Psiloglou, B. E., Giannakopoulos, C., Majithia, S., & Petrakis, M. (2009). Factors affecting electricity demand in Athens, Greece and London, UK: A comparative assessment. Energy, 34(11), 1855–1863. doi:10.1016/j.energy.2009.07.033

Rosenfeld, A. H., Akbari, H., Romm, J. J., & Pomerantz, M. (1998). Cool communities: strategies for heat island mitigation and smog reduction. Energy and Buildings, 28(1), 51–62. doi:10.1016/S0378-7788(97)00063-7

Sailor, D. (1997). Sensitivity of electricity and natural gas consumption to climate in the U.S.A.—Methodology and results for eight states. Energy, 22(10), 987–998. doi:10.1016/S0360-5442(97)00034-0

Santamouris, M. (2001). Energy and Climate in the Urban Built Environment. James & James Science Publishers, London.

Santamouris, M., Papanikolaou, N., Livada, I., Koronakis, I., Georgakis, C., Argiriou, A., & Assimakopoulos, D. . (2001). On the impact of urban climate on the energy consumption of buildings. Solar Energy, 70(3), 201–216. doi:10.1016/S0038-092X(00)00095-5

Sham, S. (1986). Temperature in Kuala Lumpur and the Merging Klang Valley Conurbation.

Sham, S. (1987). Urbanization and the Atmospheric Environment in the Low Tropics.

Sham, S. (1990). Urban climatology in Malaysia: An overview. Energy and Buildings, 15(1-2), 105–117. doi:10.1016/0378-7788(90)90121-X

Shimoda, Y., Asahi, T., Taniguchi, A., & Mizuno, M. (2007). Evaluation of city-scale impact of residential energy conservation measures using the detailed end-use simulation model. Energy, 32(9), 1617–1633. doi:10.1016/j.energy.2007.01.007

SMS, S. M. S. (1985). The Biological Environment of Singapore and its neighboring countries. In Proceeding conference (pp. 50–76).

Trihamdani, A. R., Lee, H. S., Phuong, T. T. T., Kubota, T., Tanaka, T., & Matsuo, K. (2014). Effect of green strategy in Hanoi master plan on its urban climate. In International Conference of Grand Renewable Energy 2014, Tokyo, Japan, 27 Jul-1 Aug.

Van, T. T., & Bao, H. D. X. (2006). Application of thermal remote sensing on investigating feature of urban surface temperature with distribution of land cover types in Hochiminh City. Science & Technology Development, Environment, 70–74.

Van, T. T., & Bao, H. D. X. (2010). Study of the Impact of Urban Development on Surface Temperature Using Remote Sensing in Ho Chi Minh City, Northern Vietnam. Geographical Research, 48(1), 86–96. doi:10.1111/j.1745-5871.2009.00607.x